NSTX PPPL PRINCETON PLASMA PHYSICS LABORATORY U.S. DEPARTMENT OF ENERGY Office of Science

Density fluctuation measurement by FIReTIP for the Enhanced Pedestal H-mode on NSTX

UCDAVIS UNIVERSITY OF CALIFORNIA

K. C. Lee[1], C. W. Domier[1], N. C. Luhmann, Jr[1], R. Kaita[2], R. Maingi[3]
and the NSTX Research Team

[1] University of California at Davis,
[2] Princeton Plasma Physics Laboratory, [3] Oak Ridge National Laboratory

53th APS DPP meeting
Salt Lake City, Utah. Nov. 14-18 2011

Columbia U
CompX
General Atomics
FIU
INL
Johns Hopkins U
LANL
LLNL
Lodestar
MIT
Nova Photonics
New York U
ORNL
PPPL
Princeton U
Purdue U
SNL
Think Tank, Inc.
UC Davis
UC Irvine
UCLA
UCSD
U Colorado
U Illinois
U Maryland
U Rochester
U Washington
U Wisconsin

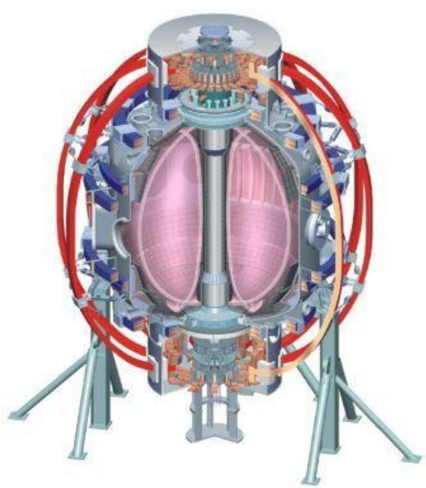

Culham Sci Ctr
U St. Andrews
York U
Chubu U
Fukui U
Hiroshima U
Hyogo U
Kyoto U
Kyushu U
Kyushu Tokai U
NIFS
Niigata U
U Tokyo
JAEA
Hebrew U
Ioffe Inst
RRC Kurchatov Inst
TRINITI
NFRI
KAIST
POSTECH
ASIPP
ENEA, Frascati
CEA, Cadarache
IPP, Jülich
IPP, Garching
ASCR, Czech Rep

Abstract

The multi-channel Far Infrared Tangential Interferometry/Polarimetry (FIReTIP) system has been used to measure changes in the electron density fluctuation spectrum for the Enhanced Pedestal H-mode (EPH-mode) on the National Spherical Torus Experiment (NSTX). Data shows dramatic density fluctuation suppression as the EPH-mode is triggered, similar in nature to the turbulence reduction present at the conventional L\H transition. Coherent fluctuations are observed by FIReTIP during the EPH-mode with frequencies greater than 10 kHz. Density fluctuation measurements from FIReTIP edge channels with different tangency radii during the EPH-mode are compared with L-mode and H-mode cases, and are presented together with a discussion of a possible EPH-mode triggering mechanism based on the gyro-center shift (GCS) theory.

******This work is supported by U.S. Department of Energy Grant Nos. DE-FG02-99ER54518 and DE-AC02-09CH11466*.**

Enhance Pedestal H-mode (EP H-mode) on NSTX

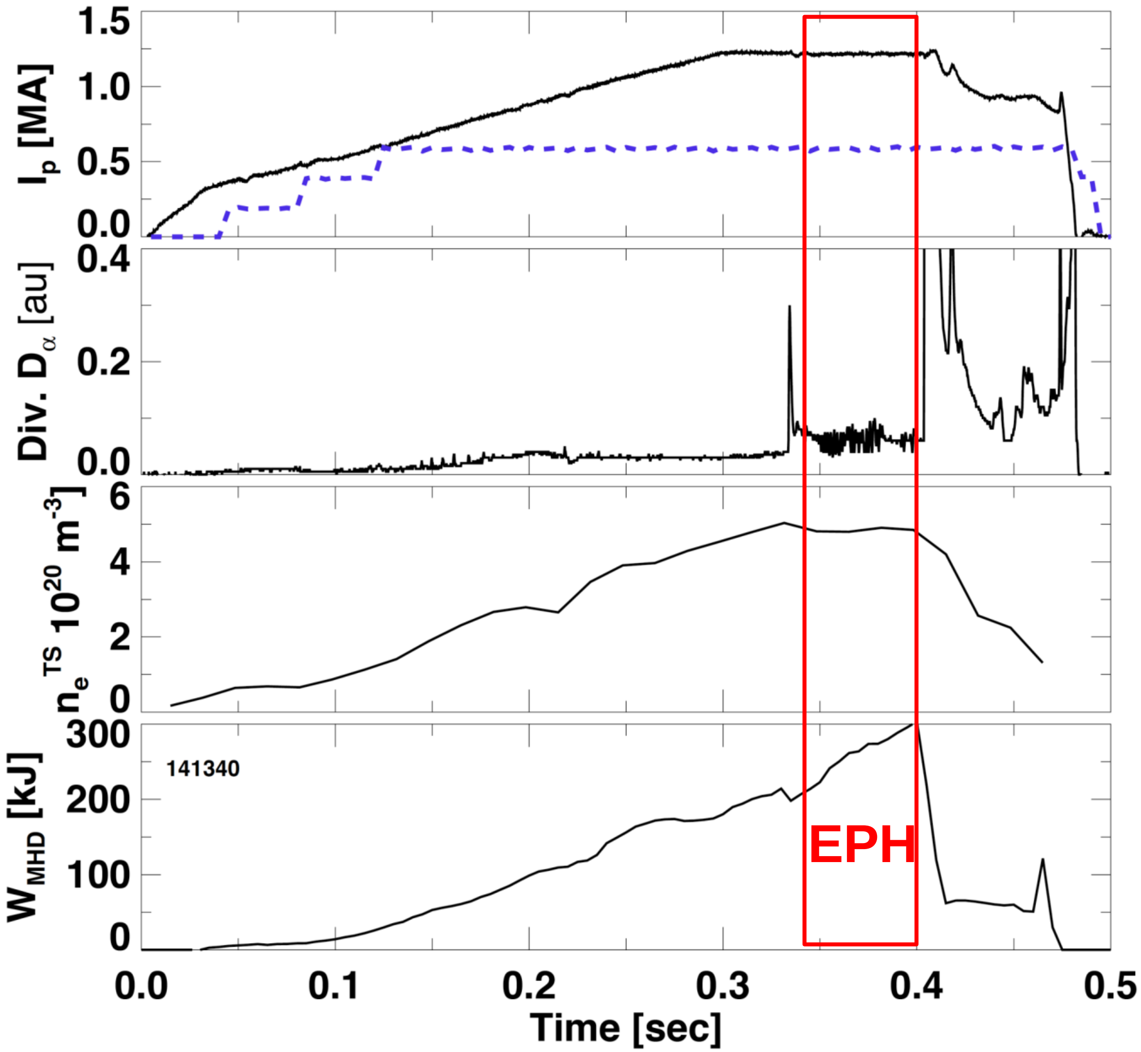

- EP H-mode triggered by natural ELM
- energy confinement increases 50%
- transition after large ELM, either natural or externally triggered by 3D fields

[R. Maingi, *et al*., PRL, **105** 135004, 2010]

Profile changes before and after the EP H-mode transition

- pedestal temperature doubles after transition
- transport barrier grows inward from the edge
- sharp pedestal correlated with toroidal velocity locked to zero near q=3 surface

transition; ~0.34 sec

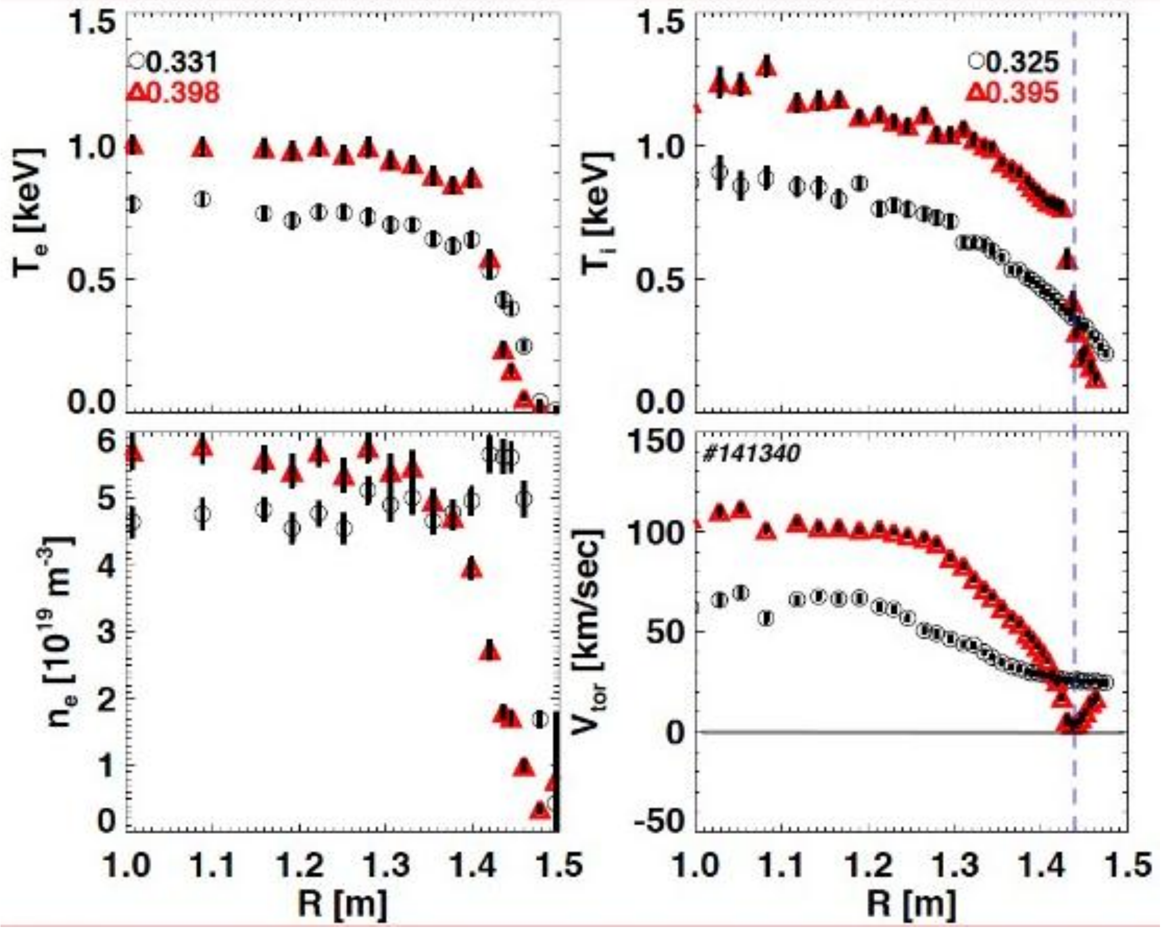

FIReTIP measurement of n_e fluctuations on NSTX

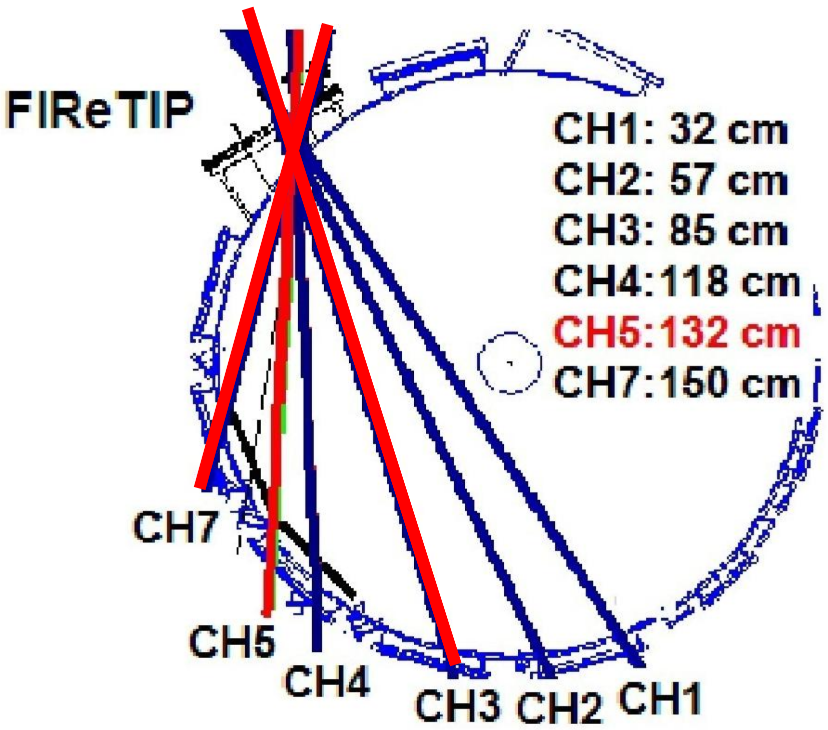

FIR interferometer

- **wavelength :119 μm**
- **bandwidth : 4 MHz**
- **two edge channels & one core channel for EPH-mode (Rt : 85 cm, 132 cm 150 cm)**

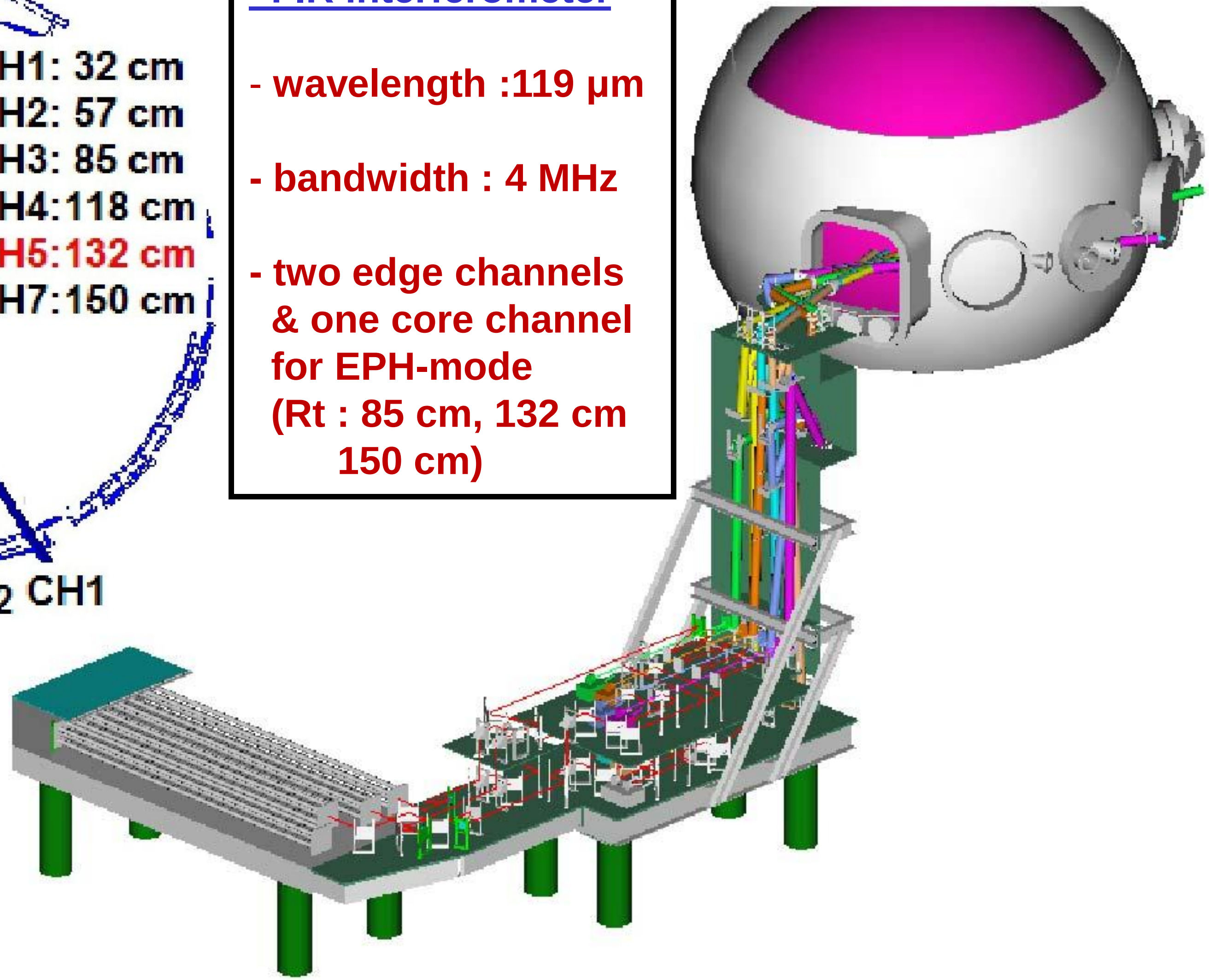

FIReTIP showed ∂n_e suppression on EPH-mode

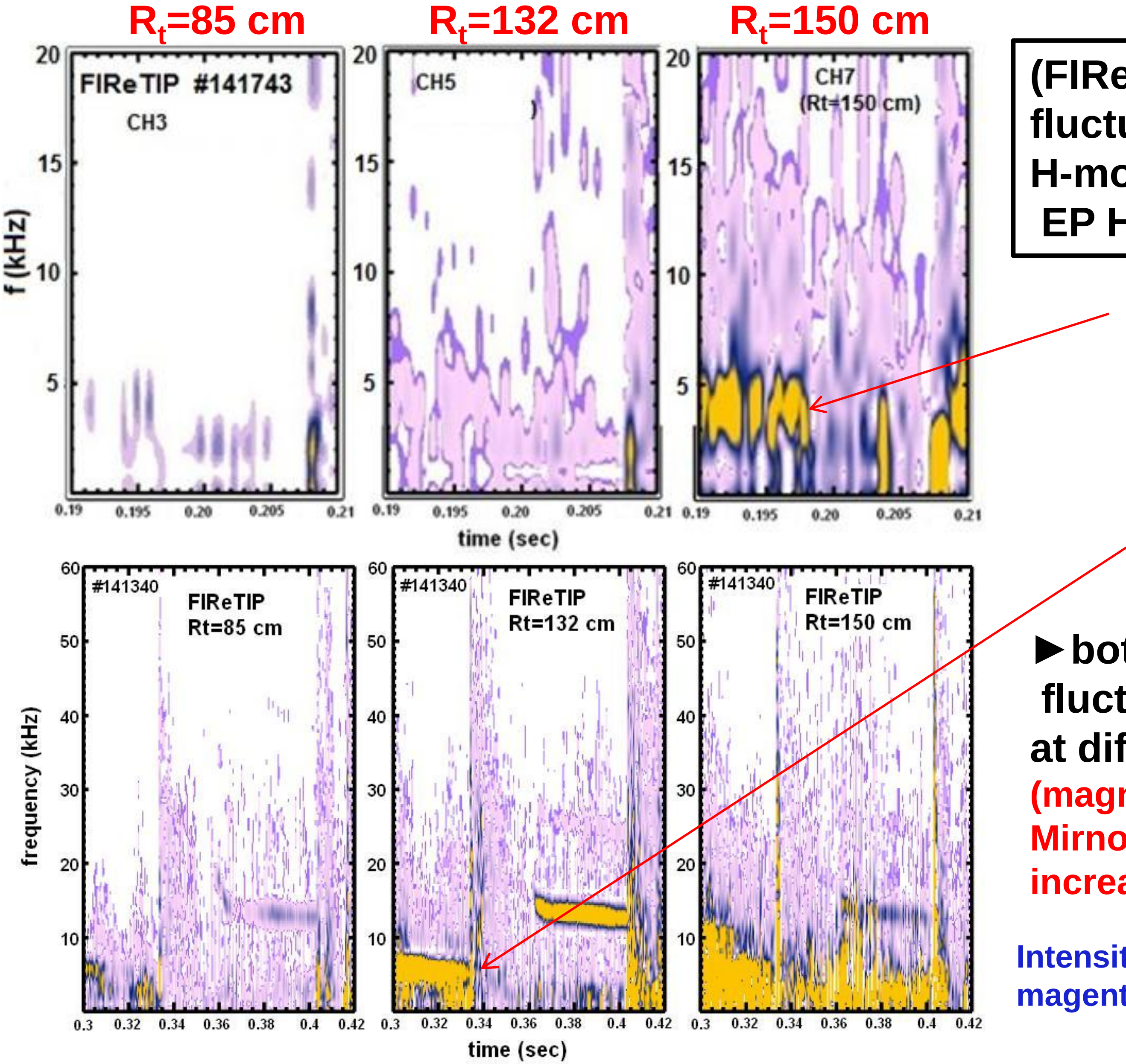

(FIReTIP) n_e fluctuation spectrum H-mode versus EP H-mode

- **both reduced fluctuations but at different location**
(magnetic fluctuations by Mirnov coil showed increase on EPH-mode?)

Intensity:
magenta < dark blue < yellow

High-k measurement also showed fluctuation reduction

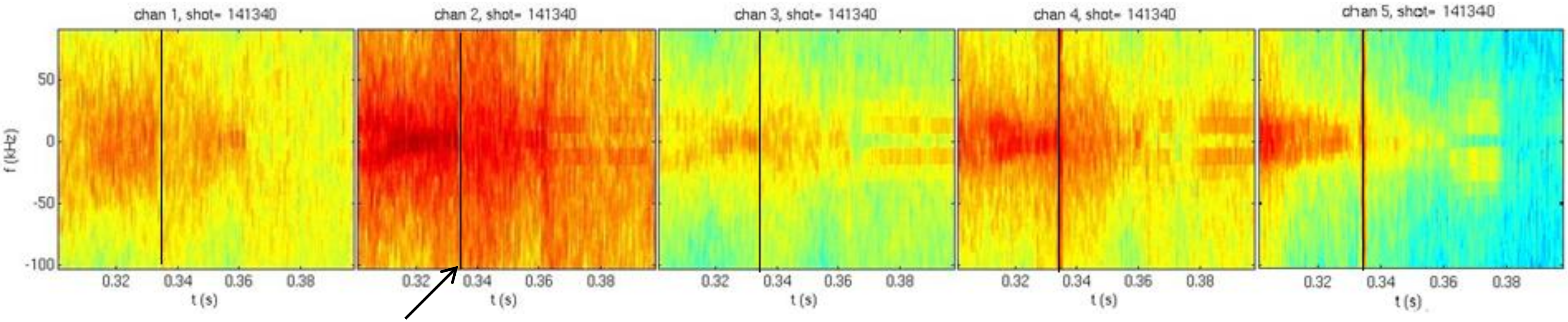

EPH-mode transition

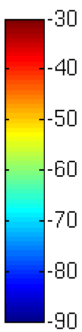

- ► measured for R_T=143-144 cm
- ► most intensive Ch2 showed clear reduction at EPH transition
- ► frequency range is similar to FIReTIP measurement

both FIReTIP and High-k showed fluctuation reduction on EPH-mode transition at few cm inner location than normal H-mode transport barrier

n_e fluctuation spectra by FIReTIP showed n=1 MHD (5~15 kHz) on EPH-mode

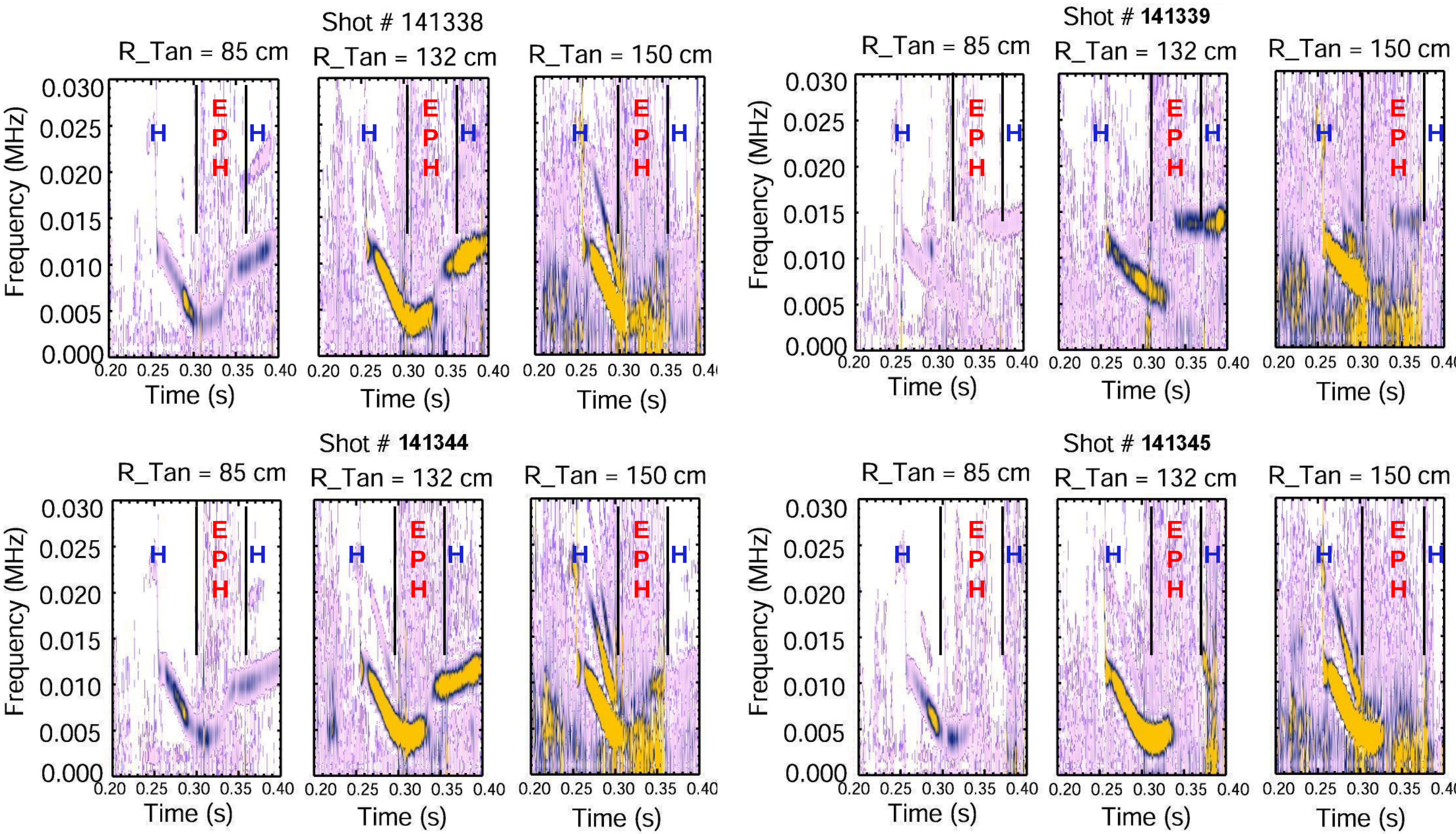

Characteristics of n=1 MHD measured by FIReTIP

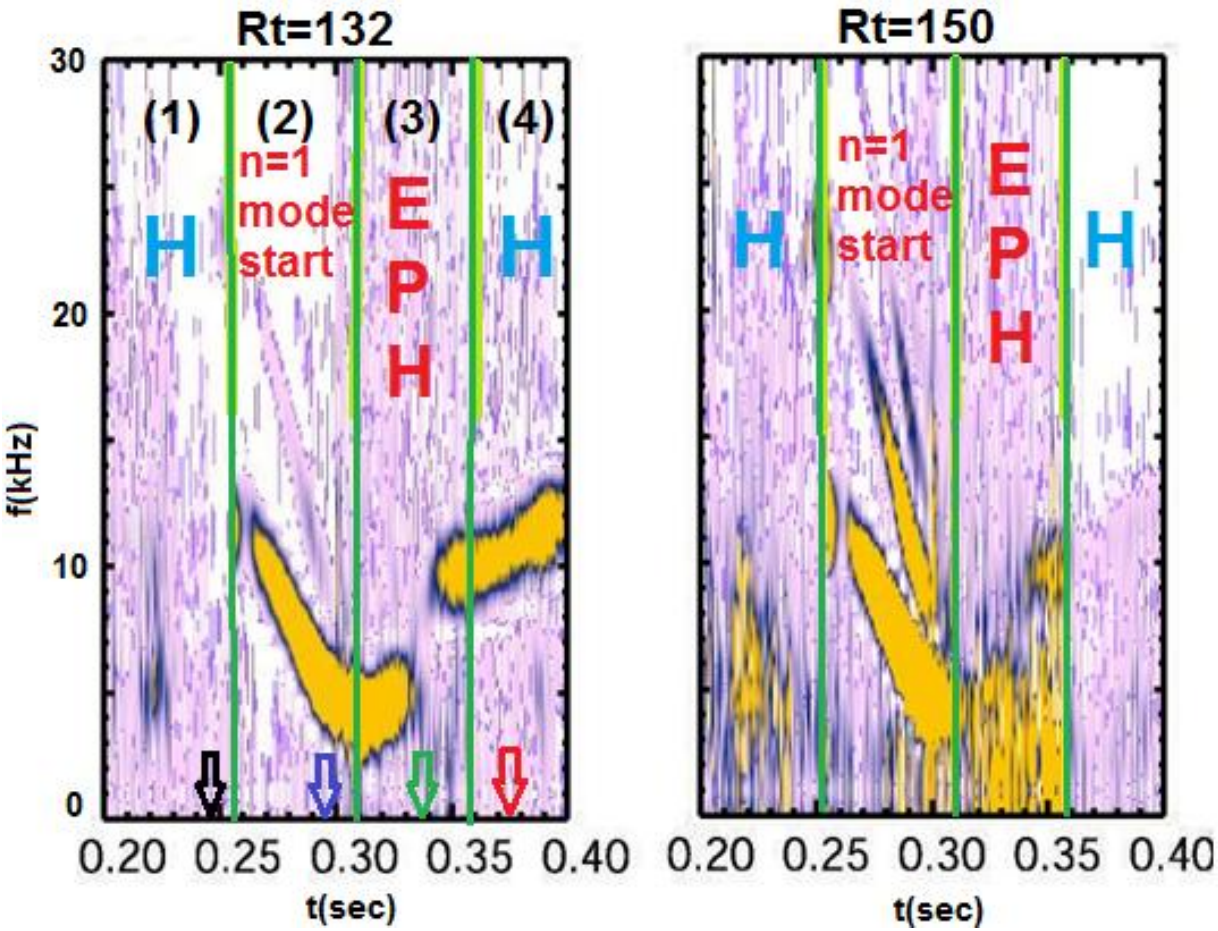

there are 4 stages:

(1) early H-mode
(2) n=1 mode start
(3) EPH-mode by ELM
(4) H-mode by ELM

► n=1 mode frequency decreases with toroidal rotation reduction in stage (2)

► on EPH-mode start by ELM, n=1 mode frequency begins to increase

► there is always n=1 mode in stage (2) but behavior of n=1 mode is not consist ant in stage (3) or (4)

V_t and E_r profile changes on EPH-mode development

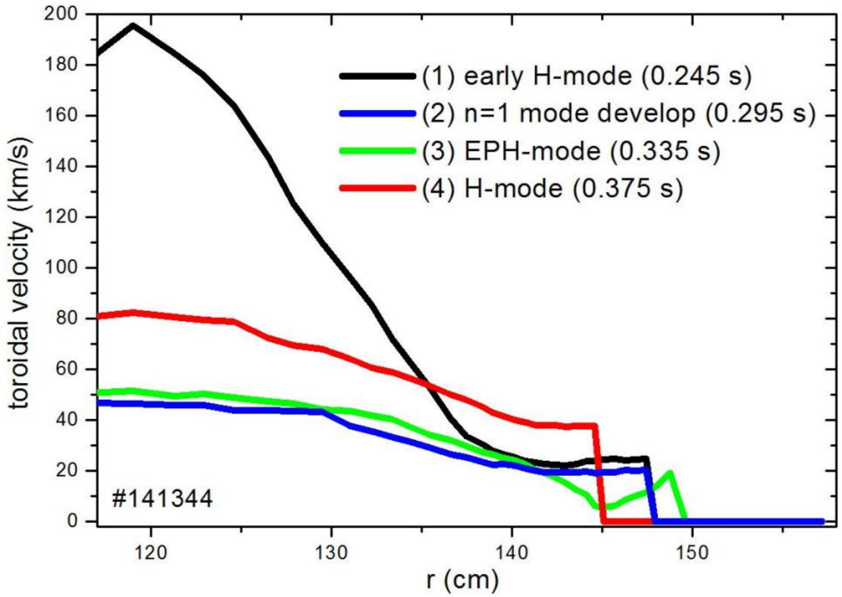

from CHERS

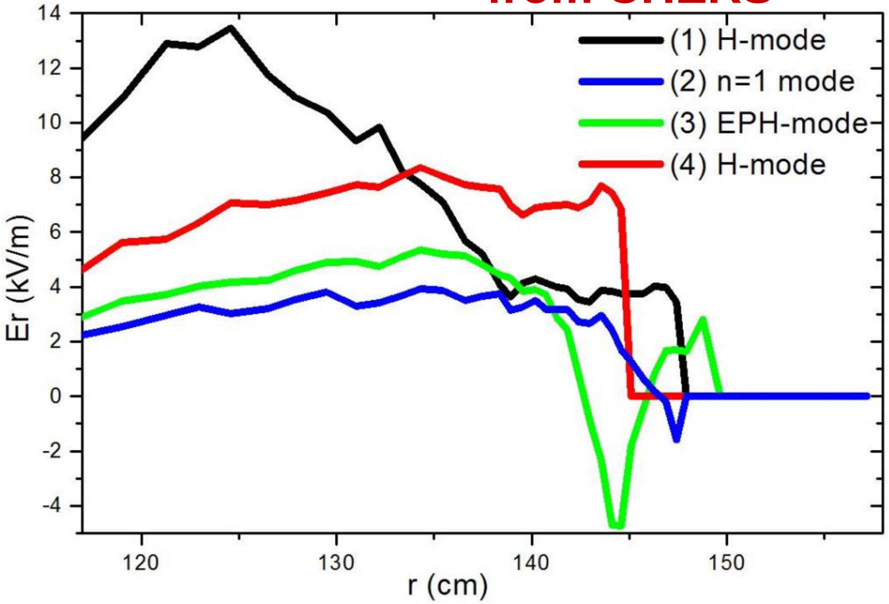

- in stage (2), while n=1 mode develops, toroidal rotation decreases, and there is additional change in Er for boundary
- by ELM, V_t and E_r profiles changed to have inside points of dip; stage (3)
- In EPH-mode, there are inflection points for E_r and V_t ($\nabla^2 E_r = 0$, $\nabla^2 V_t = 0$)
- at second ELM, EPH-mode transforms back to H-mode with inner boundary than earlier H-mode.

Theory of gyro-center shift (GCS)

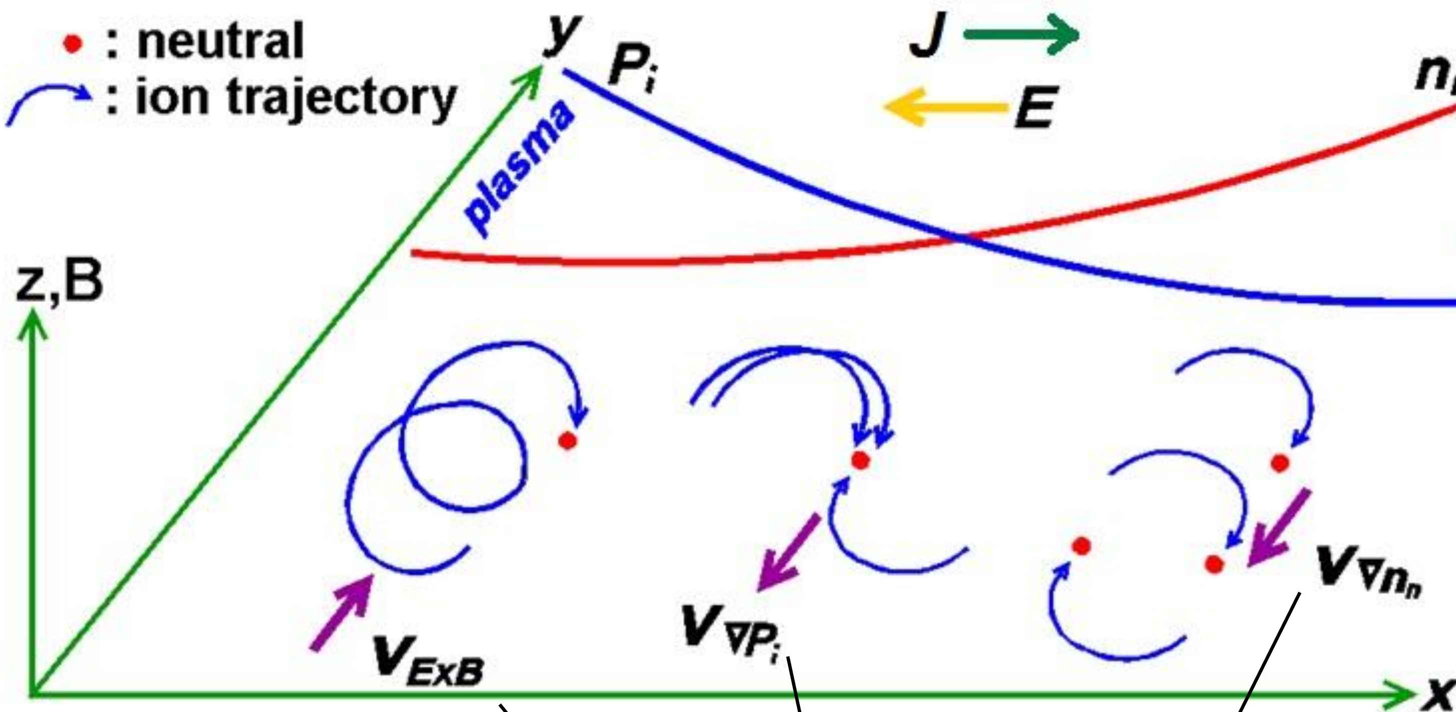

***J*x*B* =** ion momentum loss rate due to collision with neutrals

$$J_r^{GCS} = en_i \frac{r_{Li}}{\lambda_{i-n}} \left(\frac{E}{B} - \frac{1}{eB} \frac{\nabla P_i}{n_i} + \frac{kT_i}{eB} \frac{\nabla n_n}{n_n} \right)$$

return current term

driving terms

- When ions collide with neutrals, they lose their momentum; ex) charge exchange. y-components of ion velocity in above picture ($V_{\nabla p_i}$, $V_{\nabla n_n}$) generate a current in x-component (radial in tokamak) by **J**x**B** = momentum loss. $V_{\nabla p_i}$ is ion diamagnetic drift and $V_{\nabla n_n}$ is effective ion velocity comes from the neutral density gradient calculated by;

$$\upsilon_{av} = \frac{\sigma\upsilon_i \oint \upsilon n_n(x) d\theta}{\sigma\upsilon_i \oint n_n(x) d\theta} = \frac{1}{2} r_L \upsilon_\perp \frac{1}{n_n}\frac{\partial n_n}{\partial r} \quad , \quad \upsilon = \upsilon_\perp \sin\theta \hat{r} + \upsilon_\perp \cos\theta \hat{y}$$

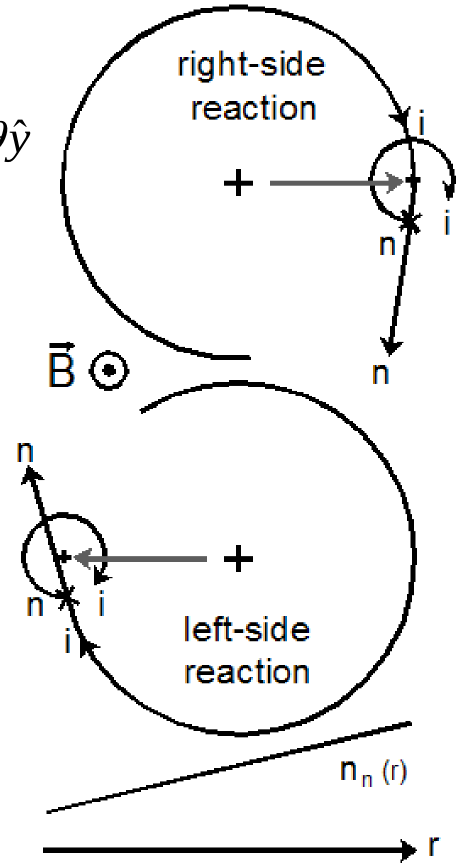

- These two terms ($V_{\nabla p_i}$,$V_{\nabla n_n}$) drive gyro-center shift current (J_r^{GCS}) and forms electric field as the source of return current.
- The theory of gyro-center shift explains the origin of the radial electric field on the boundary of tokamaks. [Lee, POP 2006]

Turbulence induced diffusion by GCS theory [Lee, PPCF 09']

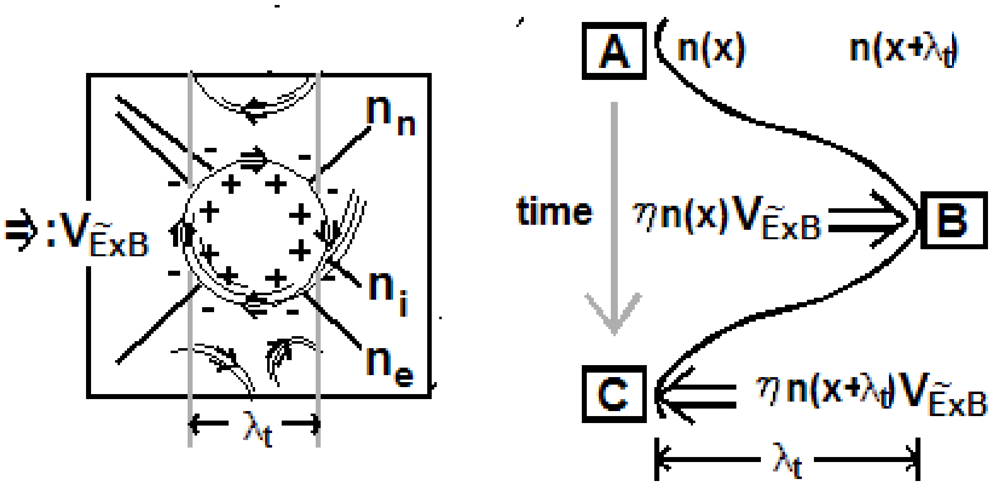

$$\Gamma = \partial n \cdot \tilde{\upsilon} \;\rightarrow\; D = \frac{\eta}{\pi}\frac{\tilde{E}\lambda_t}{B} \;\rightarrow\; D = \frac{2}{\pi}\eta^2 \frac{kT_e}{eB}$$

$\partial n = \eta\lambda_t \nabla n$, $\tilde{\upsilon} = \frac{1}{\pi}\frac{\tilde{E}}{B}$

$\tilde{E}\lambda_t \approx 2\eta \frac{kT_e}{e} \leftarrow$ ($\frac{e\tilde{\phi}_t}{kT_e} \approx \frac{\tilde{n}_e}{n_e}$: Boltzmann relation, $\tilde{\phi}_t \approx \tilde{E}\frac{\lambda_t}{2}$)

- ► turbulence induced ion and electron diffusion : $\eta\lambda_t \nabla n$
- ► turbulence induced charge diffusion : $-\eta\lambda_t \nabla\rho$
  - ► ion and electron move toward boundary => diffusion
  - ► charge (ρ) moves toward core => dilution current =>

saturation by J^{GCS}

Reynolds number of ion-neutral friction

Turbulence

- ions and electrons move toward boundary => diffusion
- charge (ρ) moves toward core => dilution current => saturation condition

$$J_r^{GCS} = en_i \frac{r_{Li}}{\lambda_{i-n}} \left(\frac{E}{B} - \frac{1}{eB}\frac{\nabla P_i}{n_i} + \frac{kT_i}{eB}\frac{\nabla n_n}{n_n} \right)$$

v*

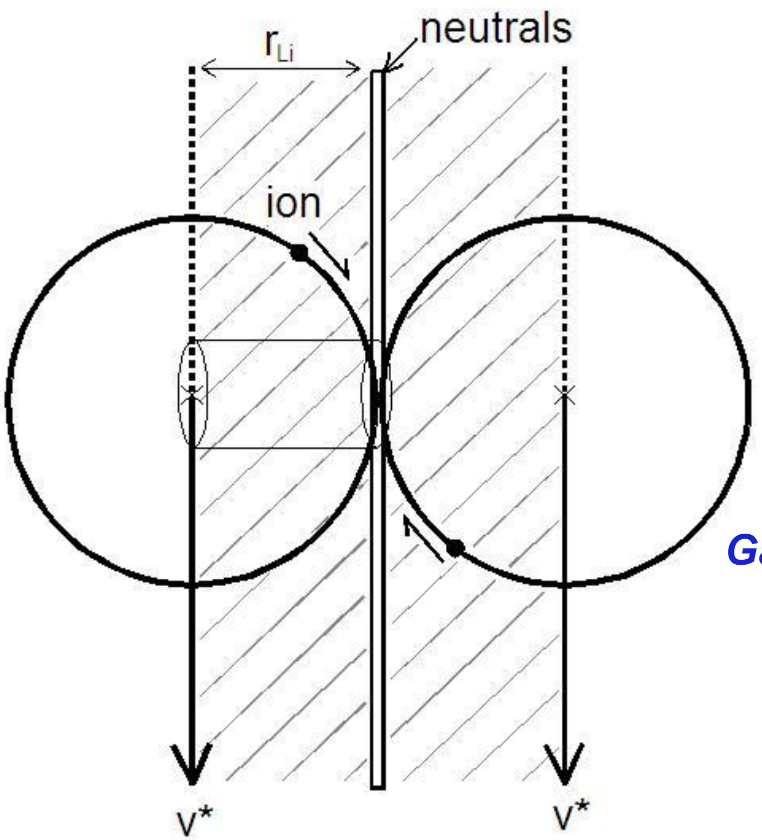

inertia force ↘

$$\mathrm{Re} \equiv \frac{n_i m_i \upsilon^{*2} / r_{Li}}{n_i m_i \nu_{i-n} \upsilon^*} = \frac{eB}{kT_i} \lambda_{i-n} \upsilon^*$$

viscosity force ↗

(saturation condition : $J_r^{GCS} = D \nabla \rho$)

$$\mathrm{Re} = \frac{2}{\pi} \eta^2 \frac{B}{m_i n_i (\sigma_{i-n} n_n)^2 \upsilon_\perp} \nabla \rho$$

Gauss's law in slab geometry $\nabla E = \frac{\rho}{2\varepsilon_0}$

$$\mathrm{Re} = \frac{4\varepsilon_0}{\pi} \eta^2 \frac{B}{m_i n_i (\sigma_{i-n} n_n)^2 \upsilon_\perp} \nabla^2 E$$

Reynolds number for EPH-mode

$$\mathrm{Re} = \frac{4\varepsilon_0}{\pi}\eta^2 \frac{B}{m_i n_i (\sigma_{i-n} n_n)^2 \upsilon_\perp} \nabla^2 E$$

If $\nabla^2 E \sim 0$, Re can be smaller than Re* which determine turbulence

Re* ≡ critical Reynolds number (2000~3000), Re < Re* (laminar, H-mode)

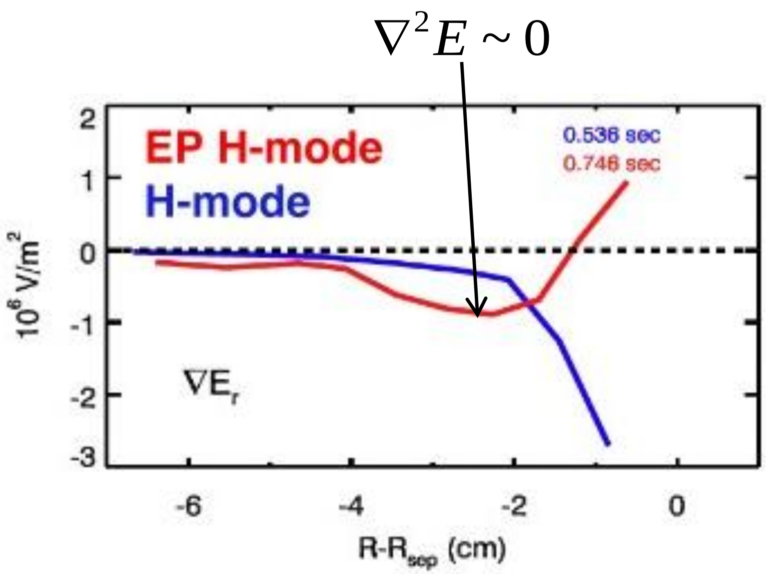

possible scenario of EPH-mode transition

ELM → change of ion velocity profile
→ change of E_r profile
→ making $\nabla^2 E \sim 0$ where inner part of H-mode transport barrier
→ Re < Re* (critical Reynolds number)
→ <u>turbulence suppression</u>
→ confinement increase

Re for H-mode and EP H-mode transitions

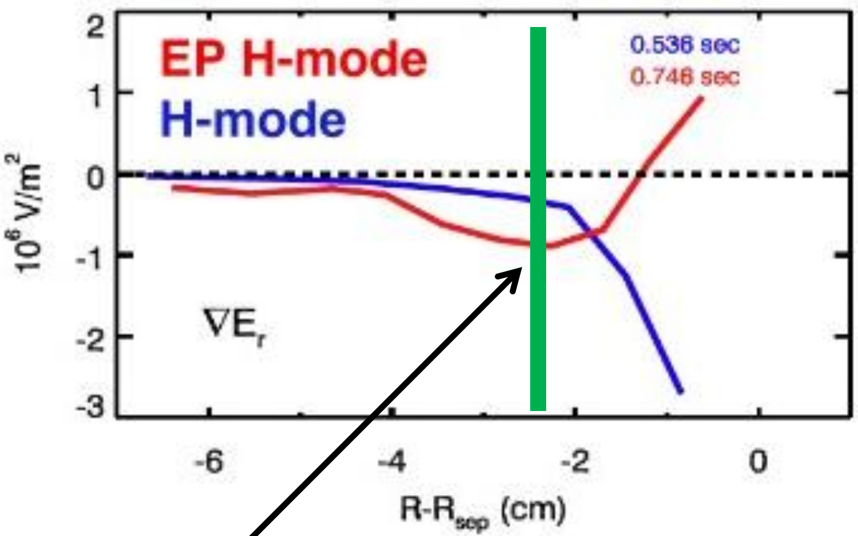

$\nabla^2 E \to 0$ **(Inflection point)**

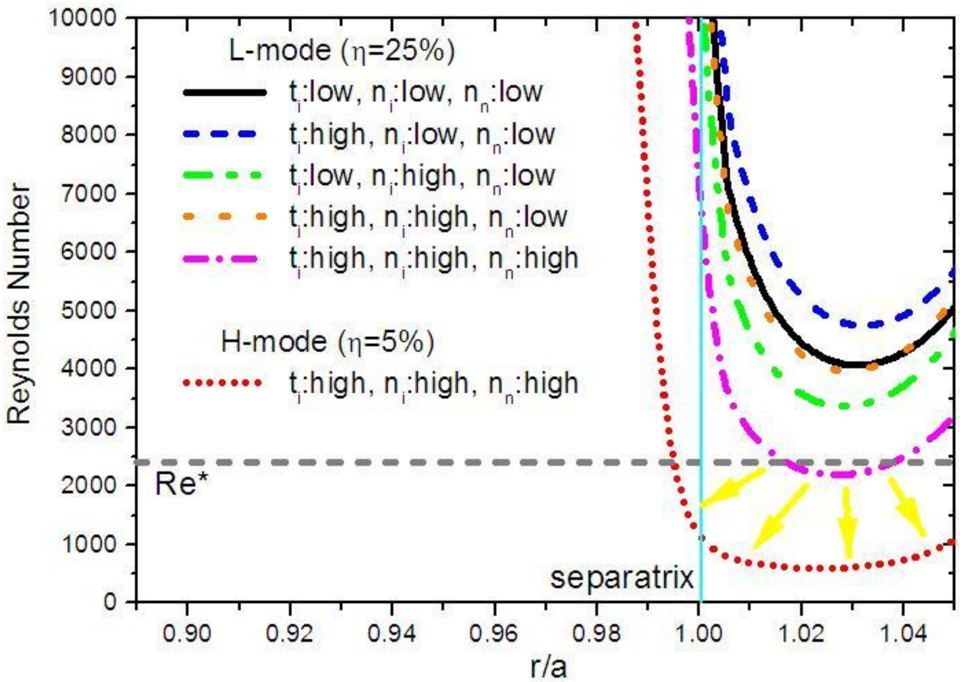

$$\mathrm{Re} = \frac{4\varepsilon_0}{\pi}\eta^2 \frac{B}{m_i n_i (\sigma_{i-n} n_n)^2 \upsilon_\perp} \nabla^2 E$$

► ***for normal H-mode,*** $|\nabla^2 E| > 0$ ***and n_n determines Re profile***

► ***for EPH-mode,*** $\nabla^2 E \to 0$ ***and Re < Re*, and n_n can be lower than H-mode***

Analysis of EPH-mode based on GCS theory

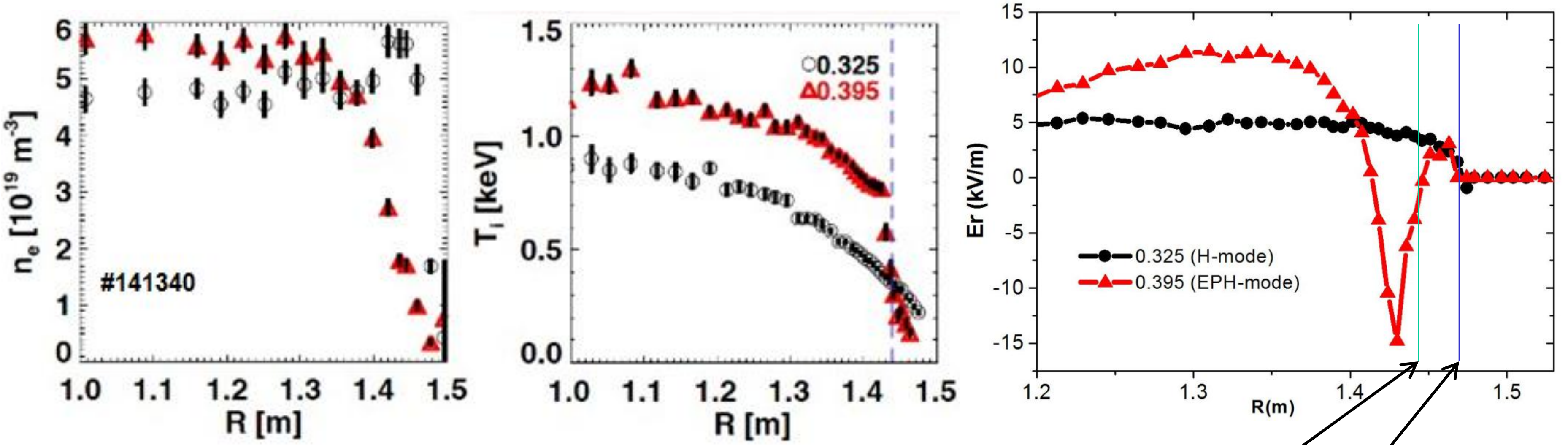

► location of EPH-mode transport barrier is close to $\nabla^2 E \rightarrow 0$ area

► transport barrier further inside of separatrix → lower neutral density

► lower neutral density → lower fueling & cooling → low n_e & high T_i

Summary

► EP H-mode is triggered by ELM and shows 50% increase of energy confinement on NSTX

► density fluctuation measurement by FIReTIP and high-k scattering system showed reduction at EP H-mode transition

► FIReTIP data showed n=1 mode development as pre-stage of EPH-mode transition.

► toroidal ion velocity and E_r profiles of EP H-mode changes to have $\nabla^2 E \to 0$ area inside of separatrix.

► Reynolds number of ion-neutral collision from gyro-center shift theory is proportional to the second gradient of E_r ($\mathrm{Re} \propto \nabla^2 E_r$)

► location of EPH-mode transport barrier is close to $\nabla^2 E \to 0$ area

► possible mechanism of EP H-mode transition :

ELM ⇨ $\nabla^2 E \to 0$ ⇨ Re < Re* ⇨ turbulence suppression

* Please e-mail to kclee@pppl.gov for reprint and further questions